Available online at www.sciencedirect.com

ScienceDirect

Procedia Engineering 99 (2015) 1213 – 1222

Procedia Engineering

www.elsevier.com/locate/procedia

"APISAT2014", 2014 Asia-Pacific International Symposium on Aerospace Technology, APISAT2014

Feasibility of an Electrostatic Energy Harvesting Device for CFCs Aircraft

Huiling Xie[a,]*, Zhaorong Huang[b], Shijun Guo[b], Ekiyor Torru[b]

[a]*Shenyang Aircraft Design & Research Institue of AVIC, 40 Tawan Street, Shenyang 110035, China*
[b]*Cranfield University, Cranfield, Bedfordshire MK43 0AL, England*

Abstract

A novel energy harvesting concept is proposed for treating local electrostatic energy produced on flying composite aircrafts. This work focuses on the feasibility research on collecting static charges with capacitive collectors. The existing energy harvesting system and the electrification of the typical carbon fibre composites (CFCs) aircraft has been reviewed. The detailed model experiments were then designed to characterize different configurations for electrostatic energy harvesting on aeroplane. In the lab, the static charge was produced by a corona discharging device, and a capacitor or a metal sheet was put in the electric field to collect the charges under four different configurations. After that, the rest results for these configurations were analysed, which is followed by the discussion about the results application on the aircraft. This work has proved that it is feasible to collect the local static electricity on flying aircraft, and it could provide a new direction of energy harvesting system in aviation field.

Peer-review under responsibility of Chinese Society of Aeronautics and Astronautics (CSAA)

Keywords: Energy harvesting; Local electrostatic; Composite aircraft; Capacitive collector

1. Introduction

When an aircraft flies through the atmosphere, electrostatic charges build up due to the interaction between the aircraft and the surrounding atmospheric environment, which has potential hazardous effects on airborne avionics

* Corresponding author. Tel.: +86-24-863-68452 ; fax: +86-24-863-68067 .
E-mail address: xie.huiling@yahoo.com

Peer-review under responsibility of Chinese Society of Aeronautics and Astronautics (CSAA)
doi:10.1016/j.proeng.2014.12.650

systems, fuelling system and human's safety. Since 1920s, aviation researchers and engineers have tried various ways to research the adverse influence of P-static on the airborne system and reduce the electrostatic hazard [1, 2]. In other words, the conventional treatments about electrostatic charges are to dissipate them.

However, in the energy harvesting field, the emerging energy harvesting researches in the aviation domain have focused on the vibration-based energy harvesting system for several years in order to provide the power supply for the wireless sensors. In a sense, this type of energy harvesting can be regarded as the process of creating energy.

In view of the points mentioned above, it is proposed an idea to connect them together. That means, the static energy accumulated during flight is a local energy, and there is no need of additional device to generate this energy. Why not collect it as a usable energy rather than only bleed off it? Based on this idea, this paper is aimed at finding an available approach to collect this local electrostatic energy which may be used as a new source of an energy harvesting system.

This paper will focus on the feasibility research on collecting static charges using capacitive collectors. The detailed practical application on aircraft is not included in this paper.

The first section of this paper investigates the existing energy harvesting system in the aviation field and the static electrification on typical carbon fiber composite aircraft. Then the second section describes the experimental design and implementation for collecting static electricity. Finally, the test results and the corresponding analysis are presented in the third section, followed by the conclusion.

2. Energy harvesting system and electrification on an aircraft

2.1. Existing energy harvesting system

In the last decade, the field of energy harvesting has attracted increasingly research interest. The applications for energy harvesters cover a wide range of civilian and military components. Out of these applications, powering wireless sensor nodes is the substantial application [3].

A typical vibration-based energy harvesting system block diagram is shown in Fig. 1. Micro power generator can collect energy from mechanical vibration. A diode AC-to-DC rectifier is used to convert the AC source to DC source. Then a DC-to-DC converter is applied to improve the energy harvesting efficiency. A stand-alone energy harvesting system with simplified control unit has been proposed by using the discontinuous conduction mode operation of DC/DC converter. Then the stable energy will be stored in batteries for powering the load like a wireless sensor [4].

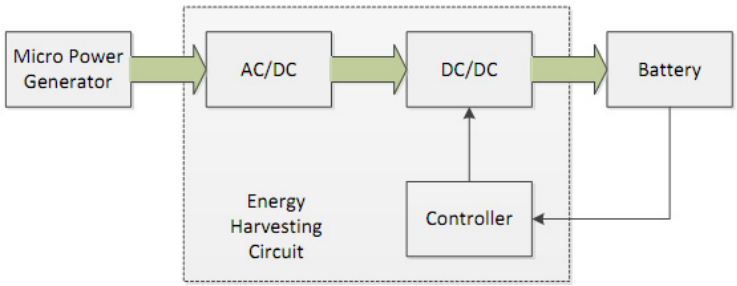

Fig. 1. Typical energy harvesting system diagram [4].

In aerospace domain, the main energy sources used as energy harvesting are vibration-based and thermoelectric energy. There are some typical practical cases described below.

For mini UAVs, energy harvesting system is an attractive technology because it can help to improve their endurance without penalty of mass or the size of fuel system. Herein some researchers used fibre based piezoceramic composite to harvest the energy and extend the flight time for UAV [5].

A vibrating structure was used to harvest strain energy for the wireless sensing system. The type of vibration-based energy harvesting system associated with the elastic strain powered wireless sensing system was implemented and tested [6].

In addition, engine's exhaust gas stream can be exploited and developed as an on-board electrical power source, which need not to move parts and can minimize the impact on fuel consumption. These engines are small, two-stroke engines which are widely used in UAV applications [7].

However, there are few published researches with respect to the local static energy utilization. P. O. Jarvinen [8] proposed an idea of an energy harvesting system sourced from P-static electrical charges during flight. These charges may be generated by the frictional charging between the precipitation particles and the external surface of the aircraft or some other factors. Another patent [9] claimed by the same author (P. O. Jarvinen) about the extra electric energy for the day-night cycle solar aircraft also described the generation of electrostatic charges by impact between the particles at the atmosphere and the flying aircraft. According to these two patents, it can be seen that the usage of electrostatic on the aircraft still remain at the conceptual stage. Hitherto there are no published documents to be found about the practical application, lab experiments or flight tests.

2.2. Principle of electrostatic on the aircraft

It is well known that the contact or friction between two objects may produce the static electricity due to the movement of electric charges. But what are the main characteristics of static electricity?

Normally, metallic material allows static charges to move freely, especially when the metal is grounded, this will make the static charges quickly move into the ground. By contrast, the static electricity cannot move in insulators, namely, if some static charges accumulate on an insulated surface, it will stay there.

Because this paper focuses on the electrostatic produced on aircrafts, this section will start from the electrification of an aircraft. In summary, there are three main causes [10] resulting in the electrostatic on aircraft:

- Frictional electrification: Generated by precipitation particles impact on the aircraft, which causes uncharged particles to be positive charged with an equal and negative charge being produced on the external surface of the aircraft.
- Engine charging: Due to the positive charge from engine exhaust expelled to the surrounding environment, which leads to the aircraft been charged with negative charges.
- Exogenous charging: Occurs when the aircraft flies through an electric field such as clouds in a thunder storm.

However, these causes mentioned above are mainly based on the metallic aircraft. How about the situation on composite aircrafts? As a matter of fact, in comparison with metal aircrafts, static electricity accumulation capacity on composite is much bigger. Moreover, the decay time for electrostatic discharging is longer. This phenomenon is mainly due to the relatively lower conductivity of composite aircraft [11].

Table 1. Typical resistivity values [12].

Material	Thickness (*cm*)	Volume resistivity (*Ohm/m*)	Surface resistivity (*Ohm/square*)	Conductivity (*Mho/m*)
Copper	0.100	1.72E-08	1.72E-05	5.81E+07
Aluminum	0.100	2.87E-08	2.87E-05	3.48E+07
GFRP (typ.)	0.100	1.80E-05	1.80E-02	5.56E+04
40% Carbon fiber	0.178	1.00E+00	5.62E+02	1.00E+00

According to [12], the material with surface resistivity less than $1 \times 10^7\ ohm/square$ has no capability to keep static charge when electrically bonded to the conductive structure. In comparison, the material that has resistivity values above $1 \times 10^{13}\ ohm/square$ can retain static charge that will not dissipate even when bonded.

The increasing widespread application of advanced composite materials in airframe causes many different problems due to their low electrical conductivity. As a matter of fact, the carbon fibre composites (CFCs) have

sufficient electrical conductivity to flow off the static electricity. So the static accumulation is not the problem for CFCs, while it is an issue for nonconductive composites [13].

2.3. Electrical characteristics of local electrostatic

Usually, the capacitance (C) of an aircraft with respect to the earth can be regarded as a constant [14], and the potential difference (V) is the value with respect to the surrounding atmosphere. In addition, for the purpose of controlling electrostatic charging, it is required that "all structural surfaces are at least mildly conductive, that all parts are electrically bonded, and that an electrical path to earth is provided" [15]. Usually the airborne systems will be grounded or bonded to main structures. And the main structures bond together in inner parts or in external parts. Because the inner surface and external surface is usually electrically conductive, the external conductive surface can be regarded as the reference ground for the airborne systems and structures. From other point of view, the aircraft is an instantaneous equipotential body with the potential everywhere on the external surface of V in a very short interval [14, 16].

According to [17] the static charge accumulation process on the surface of the aircraft during flight can be represented through following equations [17]:

$$\frac{\partial Q}{\partial \mathrm{t}} + \frac{Q}{RC} = i(\mathrm{t}) \tag{1}$$

Integrating the above equation, the static charge Q can be derived.

$$Q = I_0 RC\left(1 - e^{-t/\mathrm{RC}}\right) \tag{2}$$

Where
R = the leakage resistance of the aircraft (Ohms)
C = the capacitor for energy storage (Farads)
I_0 = the current (Amps)

The aircraft during flight can be considered as an insulated conductor with a capacitor C, so its potential voltage between the aircraft and surrounding environment can be calculated through the following equation:

$$V = \frac{Q}{C} = \frac{\int i(\mathrm{t})\mathrm{dt}}{C} \tag{3}$$

For a medium size transport aircraft, the equivalent capacitor is about 300 pF. So the aircraft potential will reach 30 kV in 1 second providing the charging current is 10μA. According to the precipitation project executed in 1945, the maximum current on the surface of an aircraft in the condition of heavy snow is around 155 μA [1], then the aircraft will reach a high voltage about 520 kV in 1 second. However, each aircraft has its own different capacitance due to different geometric shape and size, it is impossible accurately to calculate its capacitance. Usually, the estimated capacitance for an aircraft can be 1000 picofarads (1nF) [15].

3. Experimental design and lab implementation

3.1. Briefing for experimental implementation

In order to study the feasibility for collecting static charges on aeroplane using capacitive collectors, a series of model experiments were designed to characterize different configurations. A source of static charges is provided by a corona discharging device. When a high voltage is applied to the discharge terminal, a very strong electric field around the tip ionizes air molecules, and forms plasma there. The electric field then drives positive or negative

charges in the plasma towards the collecting plate. Other test devices used in the experiment include a high voltage power supply, an oscilloscope and a Multimeter. In addition, a DC power supply and the waveform generator were used in the pre-test for the designed measurement circuits. For the software used in the experiment, NI Multisim 13.0 captured and simulated circuits, while Agilent N8900A was used as an off-line oscilloscope analysis tool.

Two main different configurations of collecting capacitors were investigated for harvesting static charges, which are represented in Fig. 2. The left figure shows the configuration of collector grounded, and the collector used here was a piezoelectric actuator TH-8R. The right figure demonstrates the configuration of collector ungrounded, with the collector was a metal sheet made of copper foil. Each configuration was divided into two sub-configurations: charging with measurement load and charging without measurement load. The details of these configurations are described in 3.2 and 3.3.

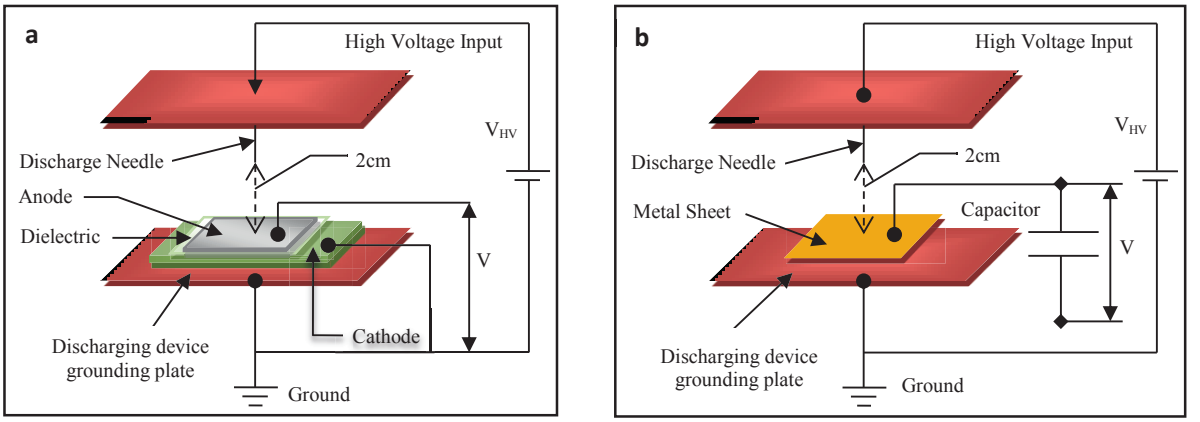

Fig. 2. (a) configuration of collector grounded; (b) configuration of collector ungrounded.

3.2. Configurations of collector grounded

In practical experiment, configuration A was tested firstly. The PZT actuator was placed between the discharge needle and the discharging device grounding plate, as shown in Fig. 2 (a). And the cathode of the PZT was connected to the grounding plate, with its anode connected to the input terminal of test circuits. Several test circuits were simulated and practically applied to find the properties of this set-up, and then a measurement circuit for source was determined; from there the final measurement circuit for configuration A was derived. Fig. 3 (a) represents the equivalent circuit of the final test circuit for configuration A. Herein C1 is the collecting capacitor with its capacitance of 30nF (here is the PZT actuator), I1 is the DC current source, C2 is a non-polarity capacitor with its capacitance of 1μF, R1 is the equivalent resistance of the oscilloscope, C3 is the equivalent capacitor of the oscilloscope, and V means the measured voltage across the anode and the cathode of the PZT via a oscilloscope. After that, a rough verification test was conducted to verify the source is really a DC current source, which utilized a current-to-voltage circuit via an operational amplifier (OPA 627 series).

However, further tests were carried out in order to verify the test set-up using a PZT actuator is reasonable and valid. A metal sheet (copper foil) replaced the PZT actuator shown in Fig. 2 (a). Then it was connected to an outside capacitor which was grounded. The potential difference across the two electrodes of the capacitor was measured in order to compare with the results (V) from previous set-up.

In comparison with configuration A, configuration B measured the voltage across the capacitor after a certain charging time rather than connecting measurement device throughout the process. The equivalent circuit is shown in Fig. 3 (b). Position 1 of the double-throw switch represents the charging process for the capacitor C1, position 2 means the discharging for the capacitor after a certain charging time. R1 in the dashed box herein is the equivalent resistance of a Multimeter.

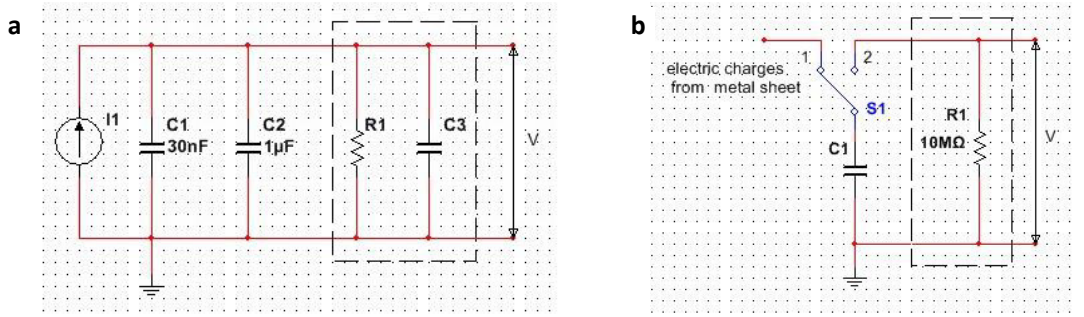

Fig. 3. (a) equivalent circuit for configuration A; (b) equivalent circuit for configuration B.

3.3. Configurations of collector ungrounded

The simplified diagram for configurations for the collector ungrounded is depicted in Fig. 2 (b). As the same with 3.2, two subcategories are included, which are described below.

Compared with configuration A, the only difference is that of the collector in configuration C is not grounded. The equivalent circuit for this configuration is shown in Fig. 4 (a). R1 in the dashed box is the equivalent resistance of the Multimeter, and it is in parallel with the capacitor which is connected to the metal sheet. The outside capacitor was a PZT (30nF) or an electrolytic capacitor (1μF).

In comparison with configuration C, the measurement load of configuration D was connected to the circuit only after a certain charging time rather than always connected to the circuit. Compared with B, the collecting capacitor was ungrounded for this configuration. The equivalent circuit for this test set-up is shown in Fig. 4 (b).

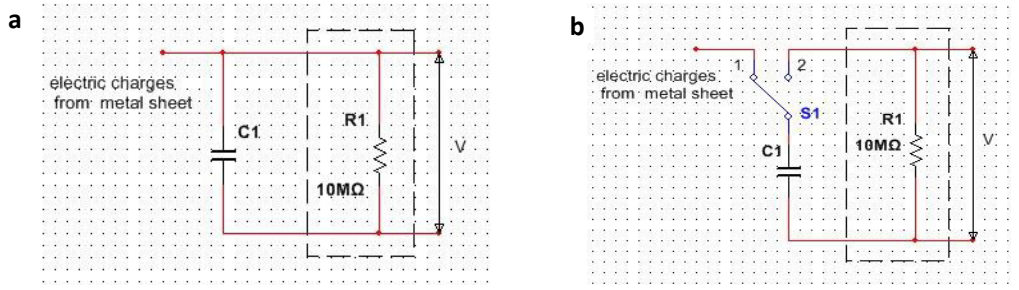

Fig. 4. (a) equivalent circuit for configuration C; (b) equivalent circuit for configuration D.

4. Test results and discussion

4.1. Test results for configuration A

Test results for four set-ups in configuration A are represented in Fig. 5 (a). It can be seen that approximately the measured initial discharge voltage at different high voltage relates to the probe ratio, and the value with probe ratio of 10:1 is about 10 times greater than the value with probe ratio of 1:1. In addition, the set-ups using a same probe could get almost the same voltage at a certain applied high voltage, no matter the combination of the capacitors. Considering the equivalent resistance of 10:1 probe is 10 times greater than that of 1:1 probe, an assumption was made: the output voltage is proportional to the load resistance. In other words, the input of the circuit can be regarded as a current source at a certain high voltage. In order to verify this assumption, a current-to-voltage conversion circuit was built and tested. Fig. 5 (b) compares verification test results to the average calculated current based on the results of Fig. 5 (a). It can be seen that, these two results are in a good agreement with each other.

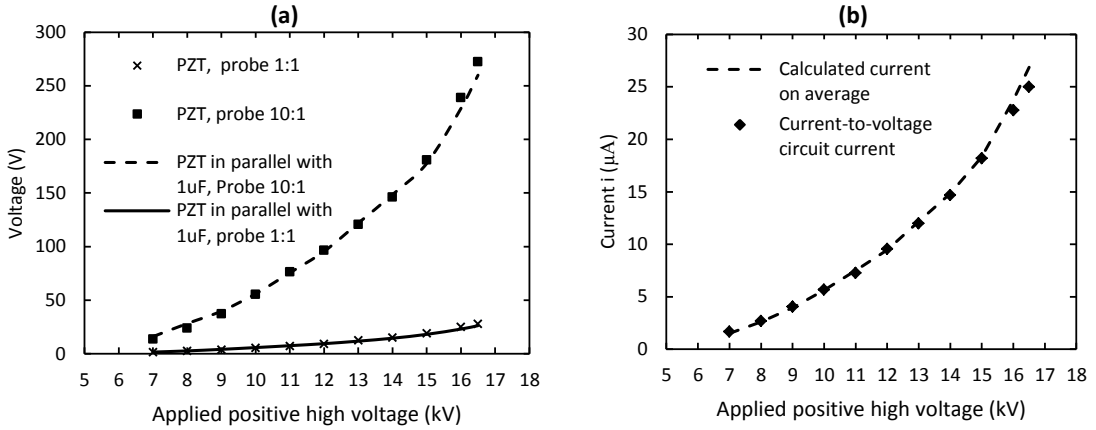

Fig. 5. (a) Test results for configuration A; (b) current source verification test result.

Based on these test results and the related test waves, two equivalent mathematical models for charging process and discharging process were derived accordingly. They can be expressed in the following equations.

$$V(\mathrm{t}) = RI_0(1 - e^{-t/\mathrm{RC}}) \tag{4}$$

$$V(\mathrm{t}) = V_0 e^{-t/\mathrm{RC}} \tag{5}$$

Where R, C, I_0, t and V in equation (4) are respectively the equivalent resistance of the circuit, the equivalent capacitance of the circuit, the assumed input current source at a certain high voltage in configuration A, the measured moment and the voltage across the capacitor C. While V_0 in equation (5) represents the initial discharge voltage at the time zero.

However, according to the comparison between the previous tests via a PZT actuator and the validity check test described in 3.2, two conclusions can be drawn as:

- The electrode of a PZT can collect the static charge in the same manner as the metal sheet does.
- The output currents are related to the material's electric conductivity and the collecting area for a same configuration.

4.2. Test results for configuration B

The fitted curves based on the test results for configuration B are plotted and shown in Fig. 6. As can be seen from this figure, the potential (V) across a capacitor is approximately proportional to the charging time. In addition, after the same charging time, the capacitor with smaller capacitance will have a higher voltage.

According to the phenomenon observed, an equivalent charging model is proposed, with its mathematical equation shown in equation (6). Herein C is the capacitor connected to the metal sheet, I is the current flowing through the capacitor and V is the voltage of the capacitor at the time of t.

It should be noticed that these two results were derived when applying same high voltage. So the currents I passing the capacitors can be assumed a same value according to 4.1. And the relationship between two capacitances and the slopes of the fitted curves in Fig. 6 can be expressed by equation (7).

$$V(\mathrm{t}) = \frac{I}{C}t \tag{6}$$

$$\frac{I/C_{PZT}}{I/C_{1\mu F}} = \frac{C_{1\mu F}}{C_{PZT}} = \frac{9.815}{0.4508} \approx 21.77 \tag{7}$$

Considering the nominal capacitance of PZT is 30nF, the estimated capacitance for the electrolytic capacitor (with its nominal capacitance is 1μF) used in the test should be 0.65μF. This value is much lower than the nominal value. It is presumed several factors contributed to this error such as ageing of the electrolytic capacitor, the unknown actual capacitance for PZT, and the manually measurement error and the like.

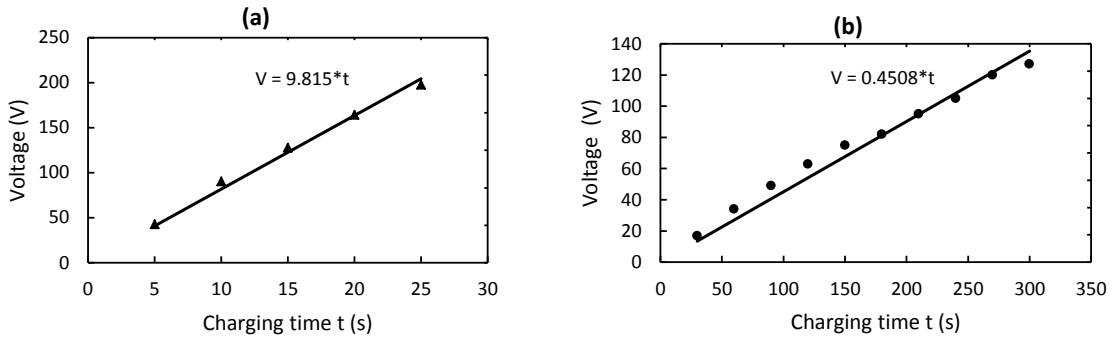

Fig. 6. (a) test result for configuration B (30nF); (b) test result for configuration B (1μF).

4.3. Test results for configuration C

The test results for configuration C is depicted in Fig. 7. As can be seen from this diagram, the variation tendency represents a similar manner with configuration A. There exists a difference in the magnitude of the measured voltage, which is mainly due to the selection of the reference zero potential. In this configuration, the zero potential is the negative electrode of the collecting capacitors, while in configuration A the real earth was selected as the zero reference. In addition, because the negative electrodes for these two capacitors are different, the reference zero potential are different accordingly, which results in the difference of the final output voltages.

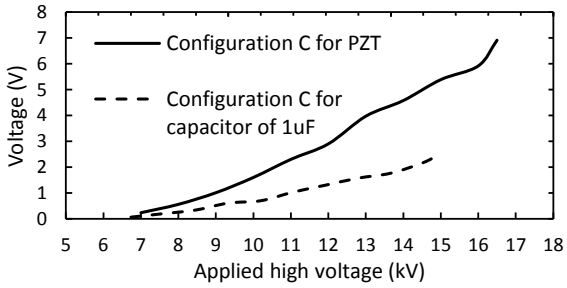

Fig. 7. Test results for configuration C

4.4. Test results for configuration D

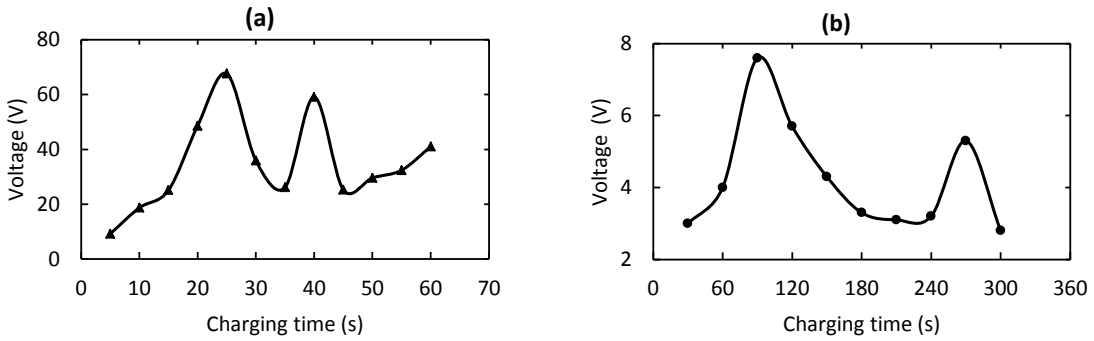

Fig. 8. (a) test result for configuration D (30nF); (b) test result for configuration D (1μF).

As can be seen from Fig. 8, the voltages of these two capacitors in configuration D show similar patterns: firstly they increase before reaching a peak, then they drop down to a certain value followed by another increasing, after that, the voltages reduce again. These results do not agree with the results obtained in configuration B. Herein there is one possible reason: the output power of the DC constant current source is limited. Namely, the DC current source provided by static electricity is not an ideal current source; therefore, the maximum output power limitation will constrain the charging process of the capacitor. However, due to the finite charging time in the experiments, it is difficult to illustrate a complete charging process in a whole time axis, so this cause needs further research.

4.5. Results application on the aircraft

By comparing the existing theoretical research described in 2.3 and the mathematical models obtained from the results analysis, it was found that the mathematical models in configurations of collecting capacitor grounded are similar to the theoretical models of the flying aircraft.

It can be seen that, if the resistance of the resistive load is not infinite, the maximum collective voltage is related to the load resistance. This situation should be the equivalent model using a serial collecting capacitor with a resistive load. One terminal of the capacitor is grounded at the conductive structure of the aircraft, while the other terminal is in charge of collecting the static charge. Taking aircraft as the reference, the charging property will be in the same manner with configuration C, or like the way of configuration A. The difference is the order of the magnitude of the collecting charge.

In comparison, in the configuration of charging without load, the collective voltage is limited by the maximum working voltage of the capacitor. This situation can be the equivalent model using a serial collecting capacitor without a resistive load. But most of the capacitors have the working voltage limitation. Even the current source generated by the static charge has an infinite output power, the capacitor can keep charging, the voltage protection circuit is still a necessity. So obviously the capacitor alone cannot accomplish the energy harvesting perfectly.

However, as mentioned before, the aircraft itself can be regarded as a capacitor and its capacitance is the value with respect to the real earth. The external surface of the aircraft is one electrode of the capacitor with the other one being the earth. And the aircraft can be regarded as an instantaneous equipotential body. So even the accumulated high voltage can reach a very high order of magnitude, the aircraft always keep zero potential level for the airborne systems and structures. In other words, this high voltage cannot be detected and hence is unusable during flight. So the electrostatic energy can be used is the currents, which may be the conduction current or the displacement current.

The current-to-voltage converter circuit used in the experiment could accomplish the conversion excellently, but whether it is suitable for the aircraft application is unknown. And the safety issues have to be considered carefully in the practical application.

5. Conclusion

According to the investigations, experiments executed and analysis for the results, the main findings and conclusions can be drawn as follows:

- Static electric properties on typical carbon-fibre composite airframe follow the same way as that of a metallic aircraft
- The configurations with grounded capacitors allow collective capacitors to harvest static charges, and have equivalent electrical properties to that of the theoretical charging process of the aircraft
- The configurations with ungrounded capacitors show different properties as compared with the configurations for grounded capacitors, but the collective capacitors in these configurations also collect static charges with much smaller magnitude
- The local electrostatic energy available on the aircraft can be regarded as a DC constant current source
- The utilization of capacitor alone will constrain the electrostatic energy harvesting due to the properties of DC current source, which requires a conversion circuit for the electrostatic energy harvesting system

Acknowledgements

The first author wishes to acknowledge Aviation Industry Corporation of China (AVIC) and China Scholarship Council (CSC) for the financial support received in 2013-14, while doing this research work at the School of Engineering (SOE) and School of Applied Science (SAS) of Cranfield University.

References

[1] R.G. Stimmel, E.H. Rogers, F.E. Waterfall, R. Gunn, Electrification of aircraft flying in precipitation areas, Proceedings of the I.R.E. and Waves and Electrons, 1946; 34: 167-177.
[2] R.L. Tanner, Radio interference from corona discharges, 1953, 591-37, Stanford Research Institute, Stanford, California.
[3] H. Kim, Y. Tadesse, S. Priya, Piezoelectric and electromagnetic energy harvesting, In: S. Priya, D.J. Inman (Eds.), Energy harvesting technologies, Springer, USA, 2009, pp. 3-4.
[4] H. Kim, Y. Tadesse, S. Priya, Piezoelectric and electromagnetic energy harvesting, In: S. Priya, D.J. Inman (Eds.), Energy havesting technologies, Springer, USA, 2009, pp.24.
[5] S.R. Anton, A. Ertuk, D.J. Inman, Energy harvesting from small unmanned air vehicles, Applications of Ferroelectrics, 2008; 3: 23-28.
[6] A. Giuliano, V. Marsic, M. Zhu, Implementation and testing of an elastic strain powered wireless sensing system for energy autonomous applications, 2012 IEEE International Conference on GreenCom, 2012; (20-23): 681-684.
[7] J. Langley, M. Taylor, G. Wagner, S. Morris, Thermoelectric energy harvesting from small aircraft engines, 2009-01-3093, SAE International, USA.
[8] P.O. Jarvinen, P-static energy source for an aircraft, 2009, US 7,592,783 B1 ed., USA.
[9] P.O. Jarvinen, Extra electric energy for day-night cycle solar aircraft, 2011, US 8,519,677 B2 ed., USA.
[10] J.E. Nanevicz, Static charging and its effects on avionics systems, IEEE Transactions on Electromagnetic Compatibility, 1982; EMC-24(2): 203-209.
[11] H. Fu, Y. Xie, J. Zhang, Analysis of corona discharge interference on antennas on composite airplanes, IEEE Transactions on Electromagnetic Compatibility, 2008; 50(4): 822-827.
[12] R.W. Evans, Design guidelines for shielding effectiveness, current carrying capacity, and the enhancement of conductivity of composite materials, 1997, NASA contractor report 4784, NASA, USA.
[13] K. Gigliotti, Static electricity and aircraft, In: Wiley Encyclopedia of Composites, 2nd ed., John Wiley & Sons, 2012, pp. 1-8.
[14] Y. Li, J. Shi, The electrostatic field characteristics of an airplane and its detection theory, Journal of detection and control, 1999; 21(4): 46-49.
[15] Department of Defense, Electromagnetic environmental effects requirements for systems, 2010, MIL-STD-464C, Department of Defense, USA.
[16] M. Yi, C. Wang, Investigation on electrostatic charge distribution and landing discharge of fixed wing aircraft, High voltage engineering, 2007; 33(7): 115-118.
[17] F. Moupfouma, N. Bae, Characterization of aircraft electrostatic charging/discharging effect and the influence of aircraft skin conductivity, 2006, 2006-01-1507, SAE International, USA.